doi:10.1093/brain/awm327 *Brain* (2008), **131**, 573–582

Probabilistic diffusion tractography of the optic radiations and visual function in preterm infants at term equivalent age

Laura Bassi,[1,2,3] Daniela Ricci,[3,4] Anna Volzone,[3,5] Joanna M. Allsop,[2] Latha Srinivasan,[2,3] Aakash Pai,[2] Carmen Ribes,[2,3,6] Luca A. Ramenghi,[1] Eugenio Mercuri,[4] Fabio Mosca,[1] A. David Edwards,[2,3,7] Frances M. Cowan,[3,7] Mary A. Rutherford[2,3,7] and Serena J. Counsell[2,7]

[1]NICU, Institute of Pediatrics and Neonatology, Fondazione IRCCS Ospedale Maggiore Policlinico, Mangiagalli e Regina Elena, University of Milan, Italy, [2]Robert Steiner MR, Unit, [3]Department of Paediatrics, Imaging Sciences Department, MRC Clinical Sciences Centre, Imperial College London, Hammersmith Campus, London, UK, [4]Paediatric Neurology Unit, Catholic University, Rome, [5]E. Medea Scientific Institute, Conegliano Research Centre, Conegliano (TV), Italy, [6]Department of Neonatology Hospital Vall d'Hebron, Barcelona, Spain and [7]Hammersmith/St Mary's Comprehensive Biomedical Research Centre, DuCane Road, London, UK

Correspondence to: Dr Serena J. Counsell, Robert Steiner MR Unit, Imaging Sciences Department, Imperial College London, Hammersmith Hospital, DuCane Road, London, W12 0HS, UK
E-mail: serena.counsell@imperial.ac.uk

Children born prematurely have a high incidence of visual disorders which cannot always be explained by focal retinal or brain lesions. The aim of this study was to test the hypothesis that visual function in preterm infants is related to the microstructural development of white matter in the optic radiations. We used diffusion tensor imaging (DTI) with probabilistic diffusion tractography to delineate the optic radiations at term equivalent age and compared the fractional anisotropy (FA) to a contemporaneous evaluation of visual function. Thirty-seven preterm infants (19 male) born at median (range) 28^{+4} (24^{+1}–32^{+3}) weeks gestational age, were examined at a post-menstrual age of 42 (39^{+6}–43) weeks. MRI and DTI were acquired on a 3 Tesla MR system with DTI obtained in 15 non-collinear directions with a *b* value of 750 s/mm^2. Tracts were generated from a seed mask placed in the white matter lateral to the lateral geniculate nucleus and mean FA values of these tracts were determined. Visual assessment was performed using a battery of nine items assessing different aspects of visual abilities. Ten infants had evidence of cerebral lesions on conventional MRI. Multiple regression analysis demonstrated that the visual assessment score was independently correlated with FA values, but not gestational age at birth, post-menstrual age at scan or the presence of lesions on conventional MRI. The occurrence of mild retinopathy of prematurity did not affect the FA measures or visual scores. We then performed a secondary analysis using tract-based spatial statistics to determine whether global brain white matter development was related to visual function and found that only FA in the optic radiations was correlated with visual assessment score. Our results suggest that in preterm infants at term equivalent age visual function is directly related to the development of white matter in the optic radiations.

Keywords: optic radiation; preterm; infant; brain; tractography

Abbreviations: DTI = diffusion tensor imaging; FA = fractional anisotropy; GA = gestational age; PMA = post-menstrual age; PVL = periventricular leucomalacia; ROI = region of interest; ROP = retinopathy of prematurity; SNR = sound-to-noise ratio; TBSS = tract-based spatial statistics

Received September 6, 2007. Revised December 4, 2007. Accepted December 12, 2007

Introduction

The incidence of preterm birth is increasing and accounts for 13% of all births in the UK. Extremely preterm infants are at high risk for neurodevelopmental impairment compared to infants born at term (Bhutta *et al.*, 2002; Marlow *et al.*, 2005), and show a higher incidence of visual

impairment that is only partly explained by retinopathy of prematurity (ROP) or brain lesions in the relevant pathways (O'Connor and Fielder, 2007). Most studies of visual function following preterm birth report visual findings after the neonatal period; at the time when more mature cortically mediated aspects of visual function (Atkinson *et al.*, 2002) can be assessed. The only studies that have systematically evaluated early visual findings in preterm infants and their correlation with brain MRI have been performed in preterm infants with periventricular leucomalacia (PVL) showing that the severity of visual impairment is associated with the extent of optic radiation injury (Eken *et al.*, 1996; Cioni *et al.*, 1997, 2000; Fazzi *et al.*, 2004; van den Hout *et al.*, 2004) and of lateral geniculate nuclei or basal ganglia involvement (Uggetti *et al.*, 1996; Ricci *et al.*, 2006). In these studies, however, visual function was assessed after the neonatal period. Less is known about the early phases of development of visual function in preterm infants.

Until recently, clinical assessments of visual function in newborns mainly consisted in evaluation of the ability to fix and follow a target, activities that are thought to be mediated by sub-cortical systems. This is based on data showing that preterm newborns even with severe occipital white matter damage can fix and follow in the first postnatal weeks. It has thus been suggested that cortical systems are not involved in these visual functions (Dubowitz *et al.*, 1986).

A recently published battery of tests for the newborn assesses additionally other aspects of visual function, including attention at distance and colour and stripe discrimination (Ricci *et al.*, 2007). This allows us to explore more complex visual responses in the period around term equivalent age and to assess whether such functions may also involve the cortical visual pathway at a time when the major influences on development will have been antenatal factors and the effects of preterm delivery.

Using Diffusion Tensor Imaging (DTI) with probabilistic tractography it is possible to delineate the white matter tracts in the different regions of the brain by determining the dominant direction of water diffusion at the microstructural level. DTI assesses the Brownian motion of water in tissue (Le Bihan *et al.*, 1986; for review Le Bihan, 2003). Water diffuses more freely parallel to white matter fibres than perpendicular to them, due to a number of factors including fibre coherence, axonal density, cell membranes and myelination (Moseley *et al.*, 1990; Beaulieu and Allen, 1994; Gulani *et al.*, 2001; Beaulieu, 2002). This directional dependence of diffusion in tissue is termed diffusion anisotropy and, by studying the preferred direction of diffusion, it is possible to infer the orientation of major white matter fibre bundles. DTI also allows for the measurement of Fractional Anisotropy (FA) (Baser *et al.*, 1994), a robust measure of microstructure that detects differences in white matter due both to maturation and damage. DTI has identified white matter microstructural abnormalities, which are not always apparent on conventional MRI, in the white matter of the preterm brain (Huppi *et al.*, 1998, 2001; Neil *et al.*, 1998; Miller *et al.*, 2002; Counsell *et al.*, 2006). In addition, probabalistic DTI tractography has proved a successful tool to assess connectivity quantitatively in preterm infants (Counsell *et al.*, 2007), delineating relevant white matter pathways on functional grounds rather than using imaging appearances. DTI thus permits a precise assessment of the optic radiations.

The aim of this study was to test the hypothesis that in preterm infants around term corrected age visual function is related to the microstructural development of white matter in the optic radiations. We measured visual abilities evaluated using a scorable clinical assessment and related this to FA in the optic radiations defined by probabilistic tractography. We took into account possible confounding by gestational age (GA) at birth, post-menstrual age (PMA) at study and the presence of MR-detectable cerebral lesions. In a secondary analysis of the DTI data, we assessed white matter microstructure throughout the brain using tract-based spatial statistics (TBSS) (Smith *et al.*, 2006) to determine whether any correlation between visual function and FA reflected local factors in the optic radiations or global white matter development.

Methods

This study was approved by the Hammersmith Hospitals Research Ethics Committee and written parental consent was obtained prior to scanning.

Subjects

We studied 37 preterm infants (19 male) who were recruited from the neonatal intensive care unit at Queen Charlotte's and Hammersmith Hospital in the early neonatal period. Infants were eligible for inclusion in this study if they were born at $\leqslant 34$ weeks GA and had no evidence of congenital anomalies, chromosomal disorders or metabolic disorders. The median [range] GA of the infants at birth was 28^{+4} [24^{+1}–32^{+3}] weeks and the median birth weight was 1.059 [0.655–1.528] kg. The infants were imaged at a median PMA of 42 [39^{+6}–43] weeks. Clinical details of the infants are given in Table 1 for the whole group and are compared between those with and without lesions on their conventional MRI scan. All infants were screened for ROP; eight were positive but none more than stage 2. All infants had a standardized visual assessment (Ricci *et al.*, 2007) on the same day as their MRI scan.

Imaging

MRI was performed on a Philips 3 Tesla system with maximum gradient strength of 62 mT/m on each independent axis and slew rate of 100 mT/m/ms on each axis using an eight-channel phased array head coil. The infants were sedated for imaging using oral chloral hydrate (30–50 mg/kg). Ear protection was used for each infant. The infant's head was immobilized using a pillow filled with polystyrene beads, from which the air was evacuated. Pulse oximetry and electrocardiograph were monitored, and a paediatrician trained in MRI procedures was in attendance throughout the examination.

Table 1 Clinical details of study group

Clinical variable	Whole cohort $n = 37$	Lesions on MRI $n = 10$	No lesions on MRI $n = 27$	Significant difference (P-value)
GA at birth in weeks, median [range]	28^{+4} [24^{+1}–32^{+3}]	28^{+4} [24^{+1}–32^{+3}]	29 [26–31^{+5}]	0.54
PMA at scan in weeks, median [range]	42 [39^{+6}–43]	42 [40^{+1}–43]	40.43 [39^{+6}–42^{+4}]	0.18
Birthweight (kg), median [range]	1.059 [0.655–1.528]	1.245 [0.616–1.44]	1.018 [0.72–1.528]	0.74
Male infants	19	7	12	0.18
Days requiring mechanical ventilation, median [range]	0 [0–12]	2 [0–12]	0 [0–7]	0.045
Days requiring CPAP, median [range]	14 [0–66]	21 [0–60]	12 [0–54]	0.96
Infants with chronic lung disease	11	3	8	0.95
Infants with culture positive post-natal sepsis	9	6	3	0.002
Infants with ROP	8 (4 stage 1, 4 stage 2)	1	7	0.28

3D MPRAGE and 3D dual echo weighted imaging was obtained prior to DTI. Single shot echo planar DTI was acquired in 15 non-collinear directions using the following parameters; TR 10 000 ms, TE 49 ms, slice thickness 2 mm, field of view 224 mm, matrix 128×128 (voxel size = $1.75 \times 1.75 \times 2\ mm^3$), b value = $750\ s/mm^2$. The data were acquired with a SENSE factor of 2.

Conventional MR images were assessed for the presence of lesions by an experienced perinatal neuroradiologist (M.A.R.).

Data analysis

Probabilistic tractography

Data analysis was performed using FSL (Smith *et al.*, 2004). Image artefacts due to eddy current distortions were minimized by registering the DT images to the b0 images using affine registration. Images were brain-extracted to remove all non-brain tissue using BET and FA maps were generated using FDT. All tractography analysis was performed by a single investigator (L.B.) while unaware of the results of visual examinations. Seed masks were positioned in the white matter lateral to the lateral geniculate nucleus, on the axial slice at the level of the transition from the posterior limb of the internal capsule to the cerebral peduncle (Ciccarelli *et al.*, 2003), on colour-coded FA maps (Fig. 1). The volumes of seed masks were standardized for all infants (9 voxels). Exclusion masks were generated to restrict the pathway to the region ipsilateral to the seed mask and posterior to the third ventricle as described by Ciccarelli *et al.* (2003). Connectivity distributions were generated from every voxel in the seed mask and were thresholded to include only those pathways with a probability of $\geqslant 10\%$; mean FA values of the connectivity distributions were determined and FA distributions were examined for normality. The analysis was repeated in 10 infants in order to determine the intra-observer variation for FA values of the optic radiations. The intraobserver variability was <2%.

TBSS

Voxel-wise statistical analysis of the FA data was carried out using TBSS implemented in FSL (Smith *et al.*, 2006). First, FA data were aligned into a common space using a non-linear registration algorithm (www.doc.ic.ac.uk/~dr/software). Then the mean FA image was created and thinned to generate a mean FA skeleton, which represented the centres of all tracts common to the group. This was thresholded to FA $\geqslant 0.15$ to include the major white matter pathways but exclude peripheral tracts where there was significant inter-subject variability and/or partial volume effects with grey matter. Each subject's aligned FA data was then projected onto this skeleton. FA data from two infants with focal lesions (one infant with middle cerebral artery infarction and one infant with periventricular haemorrhagic infarction) were excluded from this analysis due to registration errors.

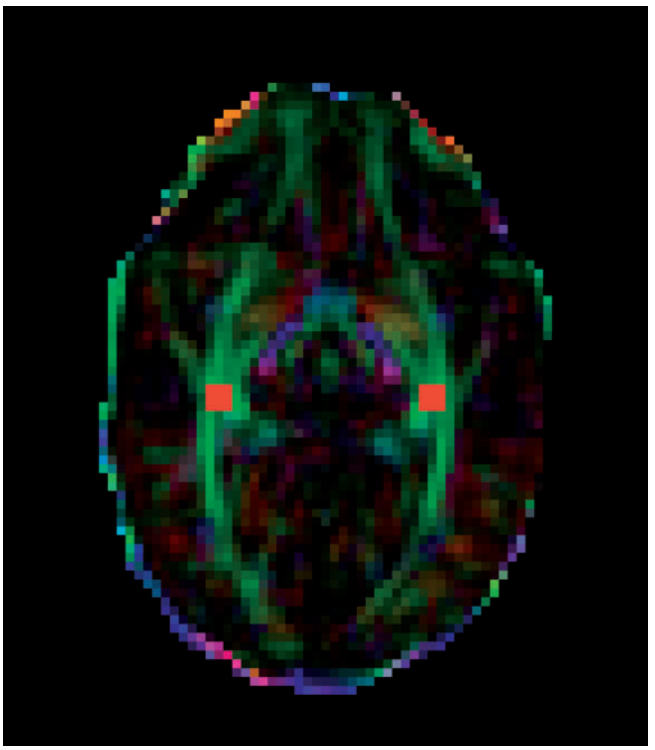

Fig. 1 Colour-coded FA map showing the position of the seed mask (in red) in the white matter adjacent to the lateral geniculate nuclei. Green represents fibres orientated in the anterior–posterior direction, blue represents fibres in the superior–inferior direction and red represents fibres in the left–right direction.

Assessment of visual function

The assessment of visual function was performed by experienced neurodevelopmental paediatricians (D.R. and A.V.) who were

Table 2 Reference data for visual assessment scores

Spontaneous ocular motility	Mainly conjugated	Occasional strabismus Occasional/lateral nystagmus	Intermittent strabismus/nystagmus	Continuous strabismus/nystagmus
Ocular movements with a target	Mainly conjugated	Occasional strabismus Occasional/lateral nystagmus	Intermittent strabismus/nystagmus	Continuous strabismus/nystagmus
Fixation	Stable (>3 s)	Unstable (<3 s)	Absent	
Tracking – black/white target				
Horizontal	Complete	Incomplete	Brief	Absent
Vertical	Complete	Incomplete	Brief	Absent
Arc	Complete	Incomplete	Brief	Absent
Colour/discrimination/attention				
Tracking coloured stimulus	Present	Absent		
Stripe discrimination	Last card identified ⩽3	4	5–6	7–8
Attention at distance	<30 cm	30–50 cm	51–69 cm	⩾70 cm

Shadowed boxes indicate the results found in 90% of full term infants at 72 h from birth.

unaware of the infants clinical history, using a battery of tests specifically designed for the early neonatal assessment of various aspects of visual function (Ricci *et al.*, 2007).

This assessment includes nine test items assessing: spontaneous ocular motility; ocular movements to a target; the ability to fix and track on a black/white target (horizontally, vertically and in an arc); the ability to track on a coloured target; to discriminate black and white stripes with increasing spatial frequency and the attention at distance evaluated as the ability to keep attention on a target moved slowly away from the infant.

The results of the assessment were scored by comparing the findings to reference data obtained in term-born infants examined 72 h after birth (Ricci *et al.*, 2007, 2007*a*). These data were obtained using the test battery in 110 term-born infants calculating the range and the distribution of frequency and the 90th centile for each item. In the present study, for each of the nine items, the findings falling within the 90th centile for term-born infants were scored as 0 while those falling outside the 90th centile were scored as 1. A total score was obtained by adding the scores of the individual items, ranging from 0 (all the items within the 90th centile) to 9 (all the items outside the 90th centile). As the items reflect nine different aspects of visual function, the total score provides an estimate of the level of visual impairment. The scoring system is shown in Table 2.

Statistical analysis

The relationship of interest was between visual score and FA in the optic radiations. Lower post-natal age at time of scan, increasing immaturity at birth and the presence of MR-detectable brain lesions are all potential confounders. Multiple regression analysis was thus specified to model the relationship between the visual function score as dependent variable and FA, GA at birth, PMA at scan and the presence of MR-detectable lesions. Partial regression plots were inspected for outliers and heteroskedacity, and residuals tested for Normality using the Shapiro–Wilkes test. Statistical analysis was performed using Stata 9.2. The relationship between visual scores and FA for the whole brain was assessed by linear regression analysis of voxel-wise cross-subject statistics using TBSS.

As ROP is known to be associated with poor visual function, FA values in the optic radiations and visual assessment scores were compared between infants who had ROP and those infants who had no evidence of ROP using a *t*-test (for FA values) or a Mann–Whitney test (for visual assessment scores).

Results

MRI

Ten infants had evidence of focal abnormalities on conventional MRI. These are described in Table 3. All 10 infants were considered to have mild or moderate ventricular dilation on qualitative visual analysis. In two infants, there were very small lesions along the optic radiation. In two others, there was mild dilation of the ventricle alongside the optic radiation. Five infants showed a degree of thalamic atrophy. Only three infants with focal lesions showed symmetrical myelination within the posterior limb of the internal capsule appropriate for preterm infants at term corrected age. For the other 27 infants, no focal abnormality was seen and the internal capsules appeared appropriately mature.

DTI

FA values in the connectivity distributions of the optic radiations in each individual infant were normally distributed, and so the mean FA value was determined. The average of all mean (±SD) FA values for the optic radiations was 0.247 ± 0.017. Figure 2 shows connectivity distributions in the optic radiations of an infant who was born at 26 weeks GA and imaged at 40 weeks PMA. There was no significant difference in FA values between the infants with and without ROP (mean FA ROP = 0.245 ± 0.021, mean FA no ROP = 0.244 ± 0.010, $P = 0.90$).

Table 3 FA values in the optic radiations and visual assessment scores in the infants with lesions on conventional MRI

Case	Ventricular dilatation	Optic radiation lesions	Thalamic atrophy	PLIC	Focal lesions	FA	Visual score
1	Mild posteriorly	Small bilateral	Minimal (Lt > Rt)	Abnormal SI bilaterally	Multiple punctate lesions in PVWM (posterior > anterior)	0.231	0
2	Mild Lt	No	Normal	Normal	Bilateral cerebellar haemorrhagic lesions	0.252	0
3	Mild Rt > Lt	No	Normal	Normal	Haemorrhagic punctate lesions in PVWM. Rt GLH	0.252	0
4	Moderate posterior > anterior	No	No atrophy. Minimal abnormal SI on Lt	Mild asymmetry Rt < Lt	Lt GLH	0.226	3
5	Mild posteriorly	No	Normal	Normal	Small cyst in Rt posterior PVWM. Small infarct Lt insula	0.239	4
6	Moderate Lt	No	Marked on Lt	Decreased myelin on Lt. No myelin on Rt	Large Lt MCA	0.226	5
7	Moderate Rt > Lt	Small lesion on Lt	Minimal on Rt	Decreased myelin	Rt caudate GLH. Lt temporal GLH	0.212	5
8	Mild posteriorly	No	Normal	Decreased myelin	Severe bilateral cerebellar haemorrhagic lesions. Vermis atrophy. Caudo-thalamic cysts	0.196	6
9	Mild Rt	No	Moderate on Rt	Abnormal myelin Rt	Rt porencephalic cyst. Rt lentiform infarct	0.217	7
10	Moderate posterior > anterior	No	Moderate bilaterally	Decreased myelin on Rt No myelin on Lt	Posterior PVWM cyst	0.204	7

GLH = germinal layer haemorrhage; Lt = left; MCA = middle cerebral artery; PLIC = posterior limb of the internal capsule; PVWM = periventricular white matter; Rt = right; SI = signal intensity.

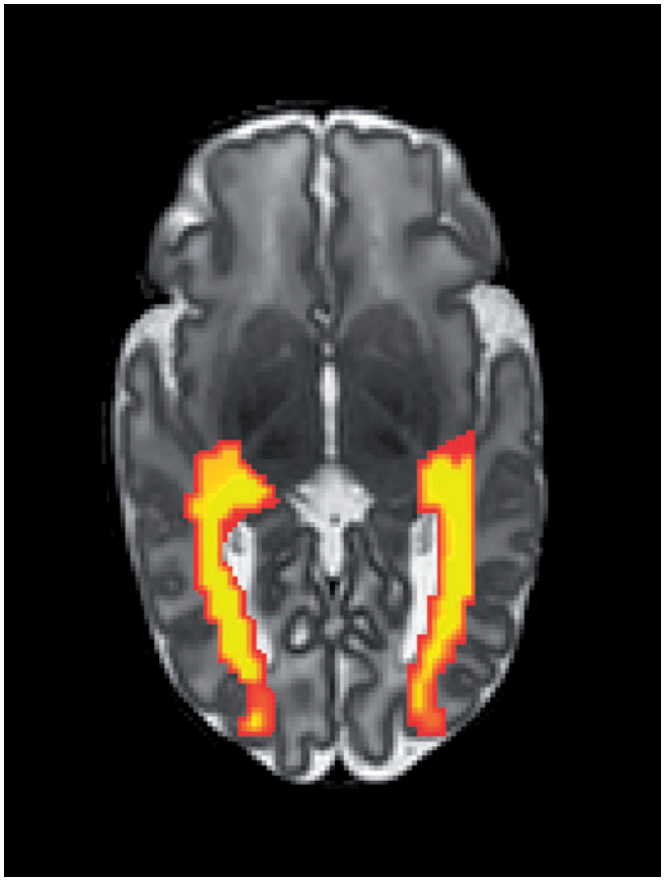

Fig. 2 Connectivity distributions in the optic radiations in an infant who was born at 26 weeks GA and imaged at 40 weeks PMA, overlaid on the infants native T_2-weighted image.

Visual assessment scores

The scores ranged between 0 (i.e. all results within the 90th centile range for our normal full term cohort) and 7. Sixteen infants had a score of 0, 7 a score of 1 and 5 a score of 2. The remaining nine had a score of $\geqslant 3$. All but two of the 27 infants without lesions had scores between 0 and 2 while 7 of the 10 infants with lesions had scores $\geqslant 3$ (Table 3). There was no significant difference in visual assessment scores between the infants with and without ROP [median (range) visual assessment score ROP = 0.5 (0–5), median (range) no ROP = 1 (0–7), $P = 0.62$]

DTI and visual function assessment

Figure 3 shows the univariate relationship between visual assessment score and FA values. Following multiple regression analysis, visual assessment score remained significantly correlated with FA values ($P < 0.001$, adjusted $r^2 = 0.669$), and GA at birth ($P = 0.60$), PMA at scan ($P = 0.85$) and the presence of lesions on conventional MRI ($P = 0.63$) did not independently predict visual performance (Table 4). Partial regression plots showed homoskedacity without significant outliers (Fig. 4), and residuals from the analysis were normally distributed. FA values in the optic radiations and visual assessment scores for the infants who had lesions on their conventional MRI are shown in Table 3.

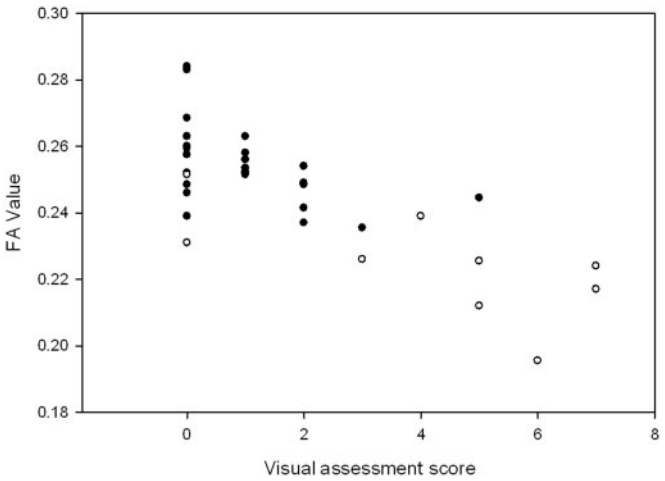

Fig. 3 Graph showing FA versus visual assessment score. Black circles indicate infants with no evidence of abnormality on MRI and white circles indicate infants with evidence of focal lesions.

TBSS

TBSS demonstrated a significant linear correlation between visual assessment scores and FA in the optic radiations (voxel-wise thresholding uncorrected for multiple comparisons, $t > 3$, $P < 0.05$). Although a few additional voxels throughout the brain demonstrated a correlation between visual score and FA, these voxels were isolated and did not correspond to any well-defined region (Fig. 5).

Discussion

This study has shown that probabilistic diffusion tractography provides quantitative information regarding white matter microstructure in the optic radiations in preterm infants at term equivalent age. FA correlated with visual assessment scores performed on the same day, and this relationship remained significant when taking into account GA at birth, PMA at scan and the presence of lesions on conventional MRI. TBSS revealed that the correlation between visual function and white matter microstructure was specific to the optic radiations and did not reflect a widespread white matter abnormality.

DTI has previously been used to assess maturational changes and to investigate white matter abnormalities in preterm infants (Huppi *et al.*, 1998, 2001; Neil *et al.*, 1998; Miller *et al.*, 2002; Counsell *et al.*, 2006; Anjari *et al.*, 2007). Most of these studies used a region-of-interest (ROI)-based approach to determine FA values at a subjectively defined site. More recently, diffusion tractography has been performed on DTI data of the preterm brain (Partridge *et al.*, 2005, 2006; Berman *et al.*, 2005; Counsell *et al.*, 2007),

Table 4 Results of multivariate analysis

Visual score	Coefficient	Standard error	*t*	*P*	95% confidence interval
FA	−88.835	19.941	−4.45	0.000	−129.454 to −48.216
GA	0.062	0.117	0.53	0.602	−0.176 to 0.299
PMA at scan	−0.041	0.214	−0.19	0.851	−0.477 to 0.396
Lesions on conventional imaging	0.334	0.687	0.49	0.630	−1.065 to 1.733

FA = fractional anisotropy; GA = gestational age; PMA post-menstrual age.

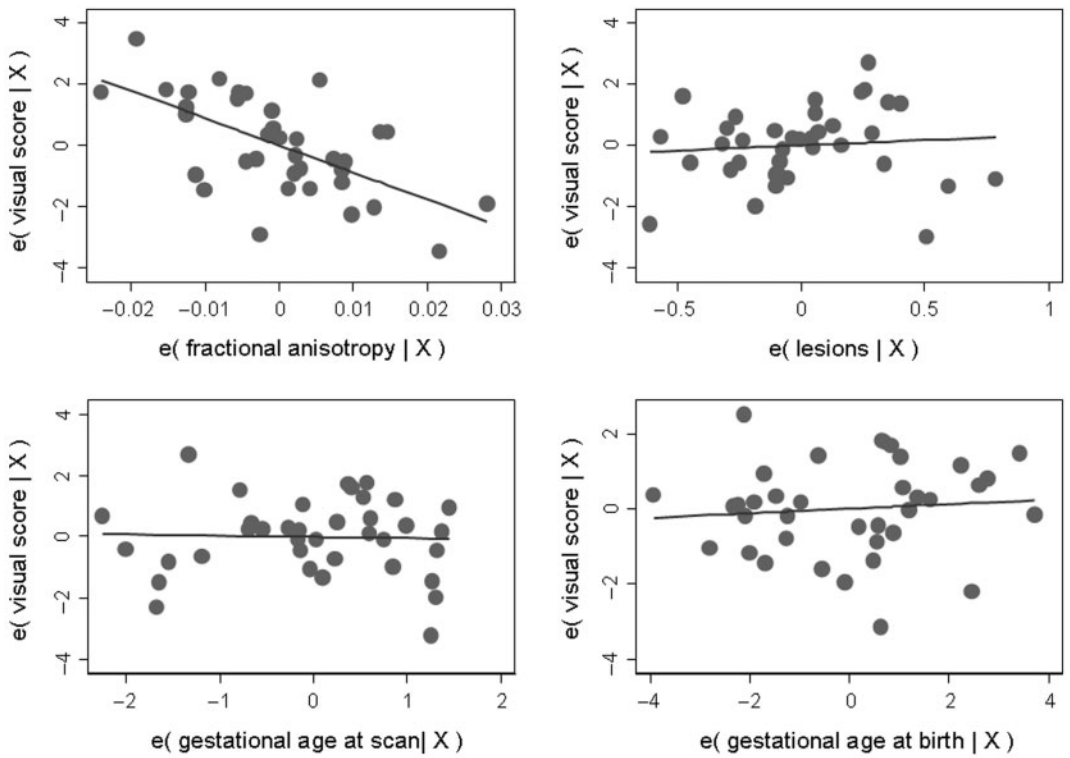

Fig. 4 Partial regression plots demonstrating the variance in (i) FA, (ii) MRI-detected brain lesions, (iii) post-menstrual age at scan, (iv) gestational age at birth attributable to the model.

and diffusion tractography has previously been used to delineate the optic radiations using streamline techniques (Yoo *et al.*, 2005; Dubois *et al.*, 2006). However, this is the first study to correlate FA values obtained from regions defined by probabilistic tractography with visual function in preterm infants at term equivalent age.

There are a number of limitations with this study. We positioned our seed mask in the white matter adjacent to the lateral geniculate nucleus, similar to the approach by Ciccarelli *et al.* (2003, 2005), as we were unable consistently to generate tracts from a seed mask positioned entirely in the lateral geniculate nucleus in these infants. Using this approach, our results were highly reproducible; nevertheless we accept our tracts may include contributions from other white matter fibre bundles such as the inferior fronto-occipital fasciculus, arcuate fasciculus and sublenticular thalamic radiation. In addition, at the resolution achievable *in vivo*, the imaging voxels will inevitably contain fibre populations with different orientations, thus the principle direction of diffusion may not be co-incident with the true orientation of the tract. However, probabilistic tractography approaches are more tolerant to this problem than streamline tractography techniques, as they allow a number of potential pathways to be considered and errant pathways, which disperse quickly, will be classified as low probability (Behrens *et al.*, 2003). Whilst our TBSS findings did not survive correction for multiple comparisons, our aim with this secondary analysis was to determine whether the correlation between visual function and FA in the optic radiations reflected a widespread white matter abnormality. The lack of correlation between other white matter regions and visual function suggests this structure–function relationship is specific to the optic radiations. Further limitations include the relatively small sample size and that we were not able to assess visual function and tractography in a control group of healthy term-born infants. We cannot,

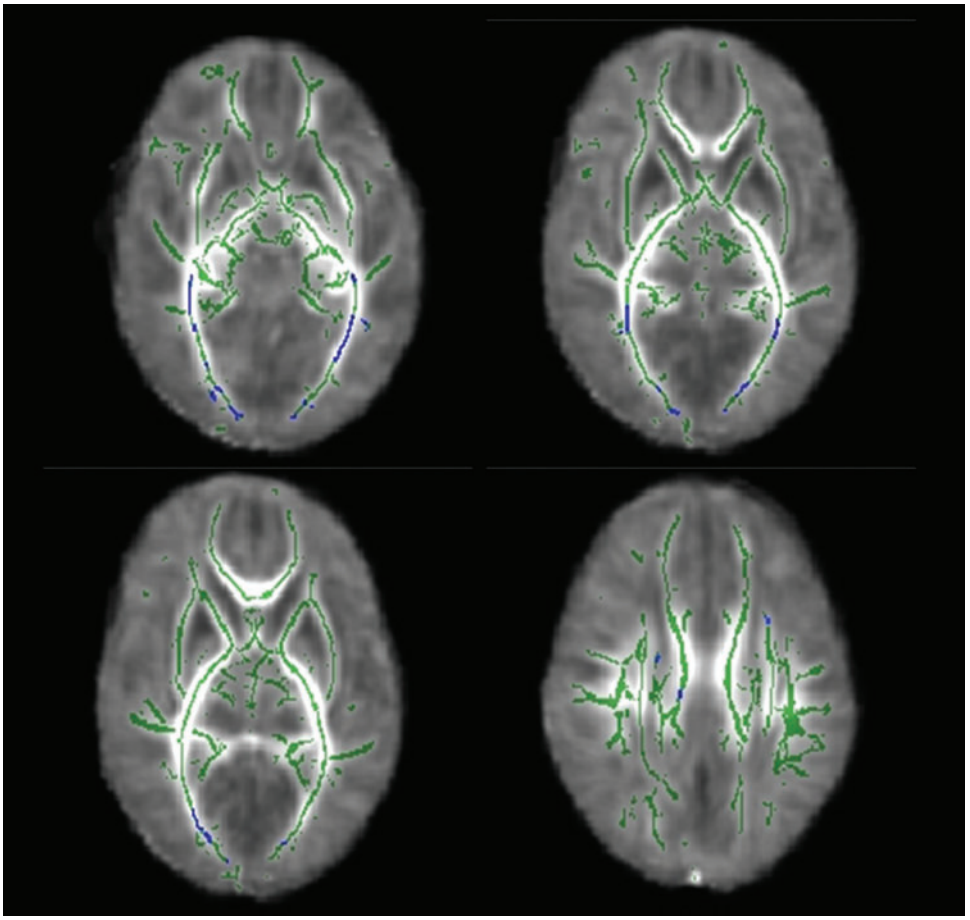

Fig. 5 Mean FA skeleton overlaid on the mean FA map. Regions of the mean FA skeleton in green represent areas where there were no significant correlation between visual scores and FA. Areas in blue are regions where visual assessment score was linearly correlated with FA.

therefore, determine whether our results are due to physiological mechanisms related to maturation or are due to pathological processes specific to the preterm population.

The use of probabilistic tractography to delineate brain structures derived from specific intracerebral connections with objective definition of ROI based on neural function represents a significant advance on subjective placements of ROI. Probabilistic approaches have the additional benefit of being able to track reproducibly through regions of relatively low FA, such as in the unmyelinated white matter of the optic radiations in these infants. Using this approach, it was possible to sample the entire tract of interest rather than an arbitrary section of that tract. Furthermore, as this study used DTI data acquired at 3 Tesla, which offers higher signal-to-noise ratio (SNR), higher spatial resolution imaging provided better depiction of tracts than could be achieved at lower field strengths (Okada *et al.*, 2006).

The results suggest that the microstructure of the optic radiations is important for visual function even in infants as young as term equivalent age. This is perhaps unexpected as at term equivalent age visual function is thought to be predominantly mediated by a subcortical visual system responsible for the early ability to fix and follow or for preferential looking (Morante *et al.*, 1982; Atkinson, 2000). The subcortical system, not only involving the lateral geniculate nucleus but also connections via thalamus and basal ganglia, appears to be essential in processing early visual information. This is based on data showing that preterm newborns even with severe occipital white matter damage can fix and follow in the first post-natal weeks suggesting that cortical systems are not involved in these visual functions (Dubowitz *et al.*, 1986). Other studies have also reported cases of relatively conserved visual function in infants with severe lesions in the occipital primary visual cortex, supporting the idea of subcortical control of early visual function mediated via extra-geniculate pathways (Aylward *et al.*, 1978; Holtzman, 1984; Snyder *et al.*, 1990). Further evidence for basal ganglia involvement comes from our studies on term-born infants with neonatal encephalopathy (Mercuri *et al.*, 1997, 1999). While infants with severe lesions in the basal ganglia but relatively preserved white matter and cortex had poor visual abilities, those with relatively large lesions involving both occipital lobes and optic radiations, especially if associated with

preserved basal ganglia and thalami had normal results on the assessment of visual function performed at 5 and 12 months and at school age. A subcortical system involving the basal ganglia has recently been suggested by functional MRI (f-MRI) studies in adults (Scholz *et al.*, 2000; Gerardin *et al.*, 2003) showing that the caudate and putamen are active during voluntary saccadic eye movements.

In the present study, not all infants with lesions or atrophy of the basal ganglia and thalami had poor visual function but often the lesions were small, unilateral and relatively anterior. The difference between our findings highlighting the involvement of optic radiations and previous studies of infants at term equivalent age may also be due to the more detailed visual assessment. Previous assessment of visual function at term corrected age have generally been limited to assessment of the ability to fix and follow and preferential looking; the battery used in this study provides other measures of visual function such as attention at distance and discrimination of colours that may reflect more mature aspects of visual processing which would implicate involvement of the cortex. Differences from previous data might also be due to the more precise analysis of the optic radiations. As there were no correlations between visual function and FA in any other white matter tract, our data suggest that low FA in the optic radiation is not a marker for widespread abnormality. Rather it implies that low FA in the optic radiation reflects local neural function and thus connection to the visual cortex. This is supported by a combined DTI and f-MRI study which demonstrated absence of the f-MRI response in the occipital cortex in an infant with extensive optic radiation injury following perinatal stroke (Seghier *et al.*, 2004).

We did not find any difference in FA values or visual assessment score in the infants who had ROP. Whilst ROP is known to be associated with poor visual function (O'Connor *et al.*, 2002), in our study cohort only 8 of the 37 infants had ROP and this was mild (either grade 1 or 2), did not require cryotherapy and had resolved by term equivalent age.

The presence of MR-detectable lesions did not predict visual performance independently of FA, but this does not imply that brain lesions may not affect visual function. Instead, it suggests that lesions influence vision through factors affecting FA in the optic radiation. Low FA values may reflect axonal degeneration, less well-organized tracts and/or delays in maturation, and may be induced by a variety of influences so these data suggest possible mechanisms for visual impairment with and without focal damage. This interpretation is supported by the observation that mean FA is lower in infants with lesions, as shown in Fig. 3.

Our results therefore suggest that even at term equivalent age the maturation and integrity of optic radiations is a major factor for the normal development of visual function in preterm infants.

Acknowledgements

We are grateful for support from the NIHR Biomedical Research Centre Funding Scheme, the NIHR post-doctoral award scheme, the Medical Research Council (UK), the Academy of Medical Sciences, The Health Foundation, Philips Medical Systems, Fondo Griffini-Miglierina of Varese and Fondazione Mariani of Italy for research grant support.

References

Anjari M, Srinivasan L, Allsop JM, Hajnal JV, Rutherford MA, Edwards AD, et al. Diffusion tensor imaging with tract-based spatial statistics reveals local white matter abnormalities in preterm infants. Neuroimage 2007; 34: 896–904.

Atkinson J. The developing visual brain. Oxford: Medical Publications; 2000. p. 65–90.

Atkinson J, Anker S, Rae S, Weeks F, Braddick O, Rennie J. Cortical visual evoked potentials in very low birthweight premature infants. Arch Dis Child Fetal Neonatal Ed 2002; 86: F28–31.

Aylward GP, Lazzara A, Meyer J. Behavioral and neurological characteristics of a hydrancephalic infant. Dev Med Child Neurol 1978; 20: 211–7.

Baser PJ, Mattiello J, Le Bihan D. Estimation of the effecive self-diffusion tensor from the NMR spin echo. J Magn Reson B 1994; 103: 247–54.

Beaulieu C. The basis of anisotropic water diffusion in the nervous system - a technical review. NMR Biomed 2002; 15: 435–55.

Beaulieu C, Allen PS. Determinants of anisotropic water diffusion in nerves. Magn Reson Med 1994; 31: 394–400.

Behrens TE, Johansen-Berg H, Woolrich MW, Smith SM, Wheeler-Kingshot CA, Boulby PA, et al. Non-invasive mapping of connections between human cortex and thalamus using diffusion imaging. Nat Neurosci 2003; 6: 750–57.

Berman JI, Mukherjee P, Partridge SC, Miller SP, Ferriero DM, Barkovich AJ, et al. Quantitative diffusion tensor MRI fiber tractography of sensorimotor white matter development in premature infants. Neuroimage 2005; 27: 862–71.

Bhutta AT, Cleves MA, Casey PH, Cradock MM, Anand KJ. Cognitive and behavioral outcomes of school-aged children who were born preterm: a meta-analysis. JAMA 2002; 288: 728–37.

Ciccarelli O, Parker GJM, Toosy AT, Wheeler-Kingshott CAM, Barker GJ, Boulby PA. From diffusion tractography to quantitative white matter tract measures: a reproducibility study. Neuroimage 2003; 18: 348–59.

Ciccarelli O, Toosy AT, Hickman SJ, Parker GJM, Wheeler-Kingshott CAM, Miller DH, et al. Optic radiation changes after optic neuritis detected by tractography-based group mapping. Hum Brain Mapp 2005; 25: 308–16.

Cioni G, Fazzi B, Coluccini M, Bartalena L, Boldrini A, van Hof-van Duin J. Cerebral visual impairment in preterm infants with periventricular leukomalacia. Pediatr Neurol 1997; 17: 331–8.

Cioni G, Bertuccelli B, Boldrini A, Canapicchi R, Fazzi B, Guzzetta A, et al. Correlation between visual function, neurodevelopmental outcome, and magnetic resonance imaging findings in infants with periventricular leucomalacia. Arch Dis Child Fetal Neonatal Ed 2000; 82: F134–40.

Counsell SJ, Shen Y, Boardman JP, Larkman DJ, Kapellou O, Ward P, et al. Axial and radial diffusivity in preterm infants who have diffuse white matter changes on magnetic resonance imaging at term-equivalent age. Pediatrics 2006; 117: 376–86.

Counsell SJ, Dyet LE, Larkman DJ, Nunes RG, Boardman JP, Allsop JM, et al. Thalamo-cortical connectivity in children born preterm mapped using probabilistic magnetic resonance tractography. Neuroimage 2007; 34: 896–904.

Dubois J, Hertz-Pannier L, Dehaene-Lambertz G, Cointepas Y, Le Bihan D. Assessment of the early organization and maturation of infants' cerebral white matter fiber bundles: a feasibility study using quantitative diffusion tensor imaging and tractography. Neuroimage 2006; 30: 1121–32.

Dubowitz LM, Mushin J, De Vries L, Arden GB. Visual function in the newborn infant: is it cortically mediated? Lancet 1986; 17: 1139–41.

Eken P, de Vries LS, van Nieuwenhuizen O, Schalij-Delfos NE, Reits D, Spekreijse H. Early predictors of cerebral visual impairment in infants with cystic leukomalacia. Neuropediatrics 1996; 27: 16–25.

Fazzi E, Bova SM, Uggetti C, Signorini SG, Bianchi PE, Maraucci I, et al. Visual-perceptual impairment in children with periventricular leukomalacia. Brain Dev 2004; 26: 506–12.

Gerardin E, Lehericy S, Pochon JB, Tezenas du Montcel S, Mangin JF, Poupon F, et al. Foot, hand, face and eye representation in the human striatum. Cereb Cortex 2003; 13: 162–9.

Gulani V, Webb AG, Duncan ID, Lauterbur PC. Apparent diffusion tensor measurements in myelin-deficient rat spinal cords. Magn Reson Med 2001; 45: 191–5.

Holtzman JD. Interactions between cortical and subcortical visual areas: evidence from human commissurotomy patients. Vis Res 1984; 24: 801–13.

Huppi PS, Maier SE, Peled S, Zientara GP, Barnes PD, Jolesz FA, et al. Microstructural development of human newborn cerebral white matter assessed in vivo by diffusion tensor magnetic resonance imaging. Pediatr Res 1998; 44: 584–90.

Huppi PS, Murphy B, Maier SE, Zientara GP, Inder TE, Barnes PD, et al. Microstructural brain development after perinatal cerebral white matter injury assessed by diffusion tensor magnetic resonance imaging. Pediatrics 2001; 107: 455–60.

Le Bihan D, Breton E, Lallemand D, Grenier P, Cabanis E, Laval-Jeantet M. MR imaging of intravoxel incoherent motions: application to diffusion and perfusion in neurologic disorders. Radiology 1986; 161: 401–7.

Le Bihan D. Looking into the functional architecture of the brain with diffusion MRI. Nat Rev Neurosci 2003; 4: 469–80.

Marlow N, Wolke D, Bracewell MA, Samara M. Neurologic and developmental disability at six years of age after extremely preterm birth. N Engl J Med 2005; 352: 9–19.

Mercuri E, Atkinson J, Braddick O, Anker S, Cowan F, Rutherford M, et al. Basal ganglia damage and impaired visual function in the newborn infant. Arch Dis Child Fetal Neonatal Ed 1997; 77: F111–4.

Mercuri E, Haataja L, Guzzetta A, Anker S, Cowan F, Rutherford M, et al. Visual function in term infants with hypoxic-ischaemic insults: correlation with neurodevelopment at 2 years of age. Arch Dis Child Fetal Neonatal Ed 1999; 80: F99–104.

Miller SP, Vigneron DB, Henry RG, Bohland MA, Ceppi-Cozzio C, Hoffman C, et al. Serial quantitative diffusion tensor MRI of the premature brain: development in newborns with and without injury. J Magn Reson Imaging 2002; 16: 621–32.

Morante A, Dubowitz LM, Leven M, Dubowitz V. The development of visual function in normal and neurologically abnormal preterm and fullterm infants. Dev Med Child Neurol 1982; 24: 771–84.

Moseley ME, Cohen Y, Kucharczyk J, Mintorovitch J, Asgari HS, Wendland MF, et al. Diffusion-weighted MR imaging of anisotropic water diffusion in cat central nervous system. Radiology 1990; 176: 439–45.

Neil JJ, Shiran SI, McKinstry RC, Schefft GL, Snyder AZ, Almli CR, et al. Normal brain in human newborns: apparent diffusion coefficient and diffusion anisotropy measured by using diffusion tensor MR imaging. Radiology 1998; 209: 57–66.

O'Connor AR, Fielder AR. Visual outcomes and perinatal adversity. Semin Fetal Neonatal Med 2007; 12: 408–14.

O'Connor AR, Stephenson T, Johnson A, Tobin MJ, Moseley MJ, Ratib S, et al. Long-term opthalmic outcome of low birth weight children with and without retinopathy of prematurity. Pediatrics 2002; 109: 12–18.

Okada T, Miki Y, Fushimi Y, Hanakawa T, Kanagaki M, Yamamoto A, et al. Diffusion-tensor fiber tractography: intraindividual comparison of 3.0-T and 1.5-T MR imaging. Radiology 2006; 238: 668–78.

Partridge SC, Mukherjee P, Berman JI, Henry RG, Miller SP, Lu Y, et al. Tractography-based quantitation of diffusion tensor imaging parameters in white matter tracts of preterm newborns. J.Magn Reson Imaging 2005; 22: 467–74.

Partridge SC, Vigneron DB, Charlton NN, Berman JI, Henry RG, Mukherjee P, et al. Pyramidal tract maturation after brain injury in newborns with heart disease. Ann Neurol 2006; 59: 640–51.

Ricci D, Anker S, Cowan F, Pane M, Gallini F, Luciano R, et al. Thalamic atrophy in infants with PVL and cerebral visual impairment. Early Hum Dev 2006; 82: 591–5.

Ricci D, Cesarini L, Groppo M, De Carli A, Gallini F, Serrao F, et al. Early assessment of visual function in full term newborns. Early Hum Dev 2007; 18: [Epub ahead of print].

Ricci D, Romeo DMM, Serrao F, Cesarini L, Gallini F, Cota F, et al. Application of a neonatal assessment of visual function in a population of low risk full-term newborn. Early Hum Dev 2007a; 7: [Epub ahead of print].

Seghier ML, Lazeyras F, Zimine S, Maier SE, Hanquinet S, Delavelle J, et al. Combination of event related fMRI and diffusion tensor imaging in an infant with perinatal stroke. Neuroimage 2004; 21: 463–72.

Scholz VH, Flaherty AW, Kraft E, Keltner JR, Kwong KK, Chen YI, et al. Laterality, somatotopy, and reproducibility of the basal ganglia and motor cortex during motor tasks. Brain Res 2000; 879: 204–15.

Smith SM, Jenkinson M, Johansen-Berg H, Rueckert D, Nichols TE, Mackay CE, et al. Tract-based spatial statistics: voxelwise analysis of multi-subject diffusion data. Neuroimage 2006; 31: 1487–505.

Smith SM, Jenkinson M, Woolrich MW, Beckmann CF, Behrens TE, Johansen-Berg H, et al. Advances in functional and structural MR image analysis and implementation as FSL. Neuroimage 2004; 23 (Suppl 1): S208–19.

Snyder RD, Hata SK, Brann BS, Mills RM. Subcortical visual function in the newborn. Pediatr Neurol 1990; 6: 333–6.

Uggetti C, Egitto MG, Fazzi E, Bianchi PE, Bergamaschi R, Zappoli F, et al. Cerebral visual impairment in periventricular leukomalacia: MR correlation. AJNR. Am J Neuroradiol 1996; 17: 979–85.

van den Hout BM, de Vries LS, Meiners LC, Stiers P, van der Schouw YT, Jennekens-Schinkel A, et al. Visual perceptual impairment in children at 5 years of age with perinatal haemorrhagic or ischaemic brain damage in relation to cerebral magnetic resonance imaging. Brain Dev 2004; 26: 251–61.

Yoo SS, Park HJ, Soul JS, Mamata H, Park H, Westin C, et al. In vivo visualization of white matter fiber tracts of preterm- and term-infant brains with diffusion tensor magnetic resonance imaging. Invest Radiol 2005; 40: 110–5.